

## Beyond 9+0: noncanonical axoneme structures characterize sensory cilia from protists to humans

Eva Gluenz,\* Johanna L. Höög,\*<sup>†</sup> Amy E. Smith,\* Helen R. Dawe,\*<sup>1</sup>  
Michael K. Shaw,\* and Keith Gull\*<sup>2</sup>

\*Sir William Dunn School of Pathology, University of Oxford, Oxford, UK; and <sup>†</sup>Boulder Laboratory for 3D Electron Microscopy of Cells, Department of MCD Biology, University of Colorado, Boulder, Colorado, USA

**ABSTRACT** The intracellular amastigote stages of parasites such as *Leishmania* are often referred to as aflagellate. They do, however, possess a short axoneme of cryptic function. Here, our examination of the structure of this axoneme leads to a testable hypothesis of its role in the cell biology of pathogenicity. We show a striking similarity between the microtubule axoneme structure of the *Leishmania mexicana* parasite infecting a macrophage and vertebrate primary cilia. In both, the 9-fold microtubule doublet symmetry is broken by the incursion of one or more microtubule doublets into the axoneme core, giving rise to an architecture that we term here the 9v (variable) axoneme. Three-dimensional reconstructions revealed that no particular doublet initiated the symmetry break, and moreover it often involved 2 doublets. The tip of the *L. mexicana* flagellum was frequently intimately associated with the macrophage vacuole membrane. We propose that the main function of the amastigote flagellum is to act as a sensory organelle with important functions in host-parasite interactions and signaling in the intracellular stage of the *L. mexicana* life cycle.—Gluenz, E., Höög, J. L., Smith, A. E., Dawe, H. R., Shaw, M. K., Gull, K. Beyond 9+0: noncanonical axoneme structures characterize sensory cilia from protists to humans. *FASEB J.* 24, 3117–3121 (2010). www.fasebj.org

**Key Words:** signaling • host-pathogen interaction • primary cilium • electron microscopy

CILIA ARE FUNDAMENTALLY IMPORTANT in cell morphogenesis, embryonic development, and tissue function. A general view has emerged that classifies axonemes into canonical, motile, 9 + 2, and noncanonical, immotile sensory 9 + 0 structures. The 9 + 2 cilia and flagella move fluids and particles across epithelia and facilitate protist and sperm motility. The link between 9 + 0 cilia and inherited disease energized the field again and emphasized the sensory function of 9 + 0 cilia (for a recent review see ref. 1). We show here that this general view is overly simplistic, and additional axonemal architectures associated with sensory structures should be incorporated into the prevailing models.

*Leishmania* parasites cause a spectrum of debilitating human diseases. In their sand fly vector, the *Leishmania* promastigote 9 + 2 flagellum functions in motility to

mouth parts and attachment to surfaces. The intracellular amastigote form that replicates in mammalian host macrophages is often described as “aflagellate.” A short flagellum is clearly present and likely to be of importance to the parasite (2), but there is confusion in the literature as to its architecture. Although the majority of studies report a 9 + 2 structure (3), some electron microscope images suggest a different architecture (4, 5). Using mouse macrophages infected with *Leishmania mexicana*, we analyzed the flagellum ultrastructure by serial thin section transmission electron microscopy (TEM) and electron tomography (Fig. 1; Supplemental Movies 1 and 2).

The amastigote flagellum is short (~1.5 μm), spanning the flagellar pocket, and only a small bulbous tip is exposed to the parasitophorous vacuole environment. Serial sectioning and tomography revealed that the axoneme microtubules were arranged as follows (Fig. 1A–E, G, and Supplemental Movies 1 and 2): 9 triplet microtubules in the basal body, a ring of 9 doublet microtubules in the transition zone with associated projections connecting to the flagellar membrane, 9 doublet microtubules surrounding a basal plate, 9 doublets surrounding a central electron dense core that displayed cell-to-cell variation, with 1 or 2 central singlet microtubules occasionally observed that terminated before the neck region. This basal structure was connected to a 9 + 0 doublet ring with occasional outer dynein arm-like structures. There was no extra-axonemal paraflagellar rod (PFR). More distally, the 9-fold symmetry was broken by microtubule doublets progressively occupying a more central position (Fig. 1G, H). This symmetry break occurred distal to the basal plate, but before the narrowing of the flagellar pocket neck (Fig. 1H). Serial section examination of doublet displacement in 22 axonemes showed that in 10 axonemes 1 doublet was displaced, while 2 doublets were displaced simultaneously in 12 axonemes. Thus,

<sup>1</sup> Current address: School of Biosciences, Geoffrey Pope, University of Exeter, Stocker Rd., Exeter EX4 4QD, UK.

<sup>2</sup> Correspondence: Sir William Dunn School of Pathology, University of Oxford, South Parks Road, Oxford OX1 3RE, UK. E-mail: keith.gull@path.ox.ac.uk

doi: 10.1096/fj.09-151381

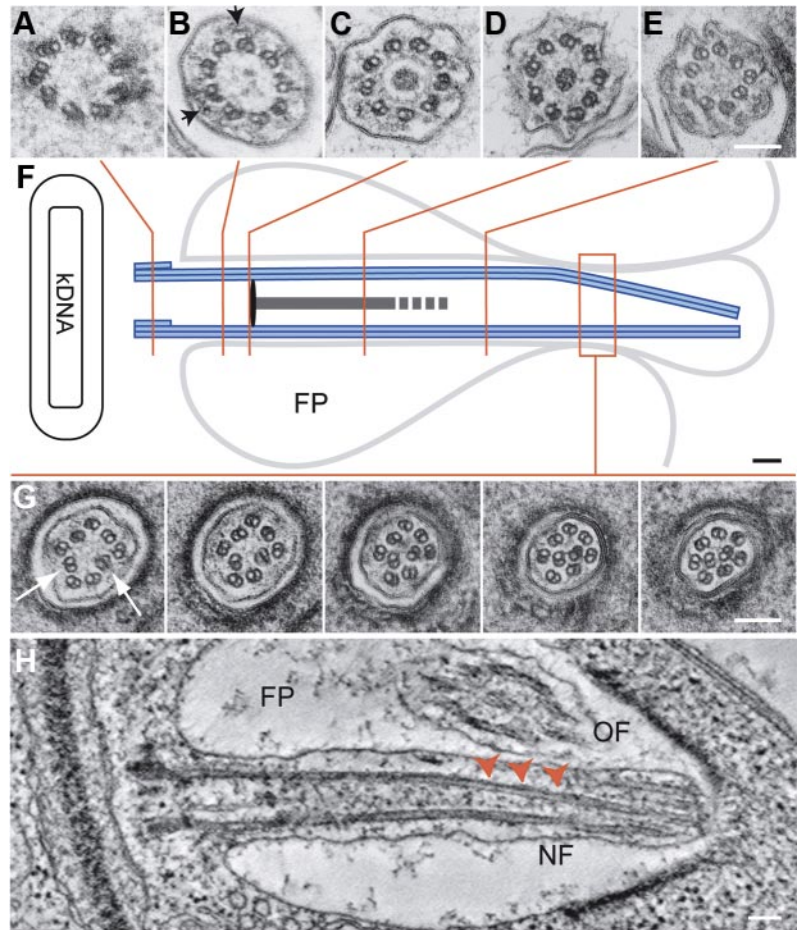


**Figure 1.** Structure of the *L. mexicana* amastigote flagellum. J774 macrophages were infected with stationary phase *L. mexicana* promastigotes (21). Three days postinfection cells were fixed and processed for TEM essentially as described previously (22). *A–E*, *G*) Arrangement of microtubules along the axoneme. Arrowheads (*B*) indicate IFT particles. *F*) Position of sections in *A–E* and *G*. *G*) Displacement of doublets (arrow) shown in serial thin sections through the distal portion. *H*) Tomographic slice from a reconstructed 3-D volume of a dividing amastigote showing the growing flagellum (NF) in longitudinal section; arrowheads indicate symmetry break. FP, flagellar pocket; OF, mature flagellum. Scale bars = 100 nm.

we conclude that the structure of the amastigote flagellum is distinct from the promastigote flagellum (a canonical 9+2 structure); however, it is strikingly reminiscent of early reports of the structure of the vertebrate primary cilium.

Although the vertebrate primary cilium is generally described as 9 + 0, early TEM studies from 40 yr ago indicated that the 9 + 0 symmetry is broken soon on exit of the cilium from the cell in diverse tissues and organisms (for example, see refs. 6–8). This feature of primary cilia has not been widely acknowledged recently, and its significance remains unknown. We revisited this issue using serial thin sections of the kidney primary cilium (Fig. 2*A, B*) and found that the 9 + 0 doublet structure distal to the triplet basal body (with associated procentriole) persisted for <500 nm ( $n=18$  series). The first sign of symmetry break was a flattening of the axoneme (Fig. 2*A7*, black lines) followed by repositioning of the doublets at this position (Fig. 2*A8*, arrows). Progressive cilium tapering occurred; ultimately the axoneme contained only 1 doublet and 4 singlets. Rather than 9 + 0, we suggest that such axonemes be referred to as 9<sub>v</sub> axonemes, 9<sub>v</sub> standing for 9 variable. Variation comes in 3 particular areas (in addition to lack of central pair microtubules): bundling of the axonemal doublets, eventual reduction in doublet numbers to many less than the original 9, and eventually, in some cases, to singlet microtubules.

Interestingly, connections between the microtubule doublets and the ciliary membrane (generally indicative of the transition zone) persisted for much of the cilium length (*e.g.*, Fig. 2*A16*, inset). These were also observed in the distal portion of the *L. mexicana* amastigote flagellum (Fig. 1*G*), raising the intriguing possibility that portions of the primary cilium and possibly the amastigote axoneme should be considered as extended transition zones.

We then asked whether a specific microtubule doublet became displaced in breaking the 9-fold symmetry. This is difficult to address in mammalian systems because the lack of an extra-axonemal reference point precludes absolute doublet numbering. We assigned each doublet a letter, A–I, based on its position *relative* to the procentriole (Fig. 2*C*), and used this nomenclature to look at doublet displacement. In serial sections of 18 axonemes, 4 showed displacement of a single doublet; in the remaining 14, 2 doublets were simultaneously displaced (Fig. 2*A8, B7*; arrows). These doublets were always separated by  $\geq 2$  other doublets (Fig. 2*A, B*). No particular doublet was consistently displaced, but there was a striking preference for doublets D, E, H, and I (Fig. 2*E*).

In *Leishmania* 9 + 2 promastigote axonemes, the singular position of the PFR and the fixed position of the 2 central microtubules provide reference points for absolute doublet and triplet numbering (Fig. 2*D*; ref.

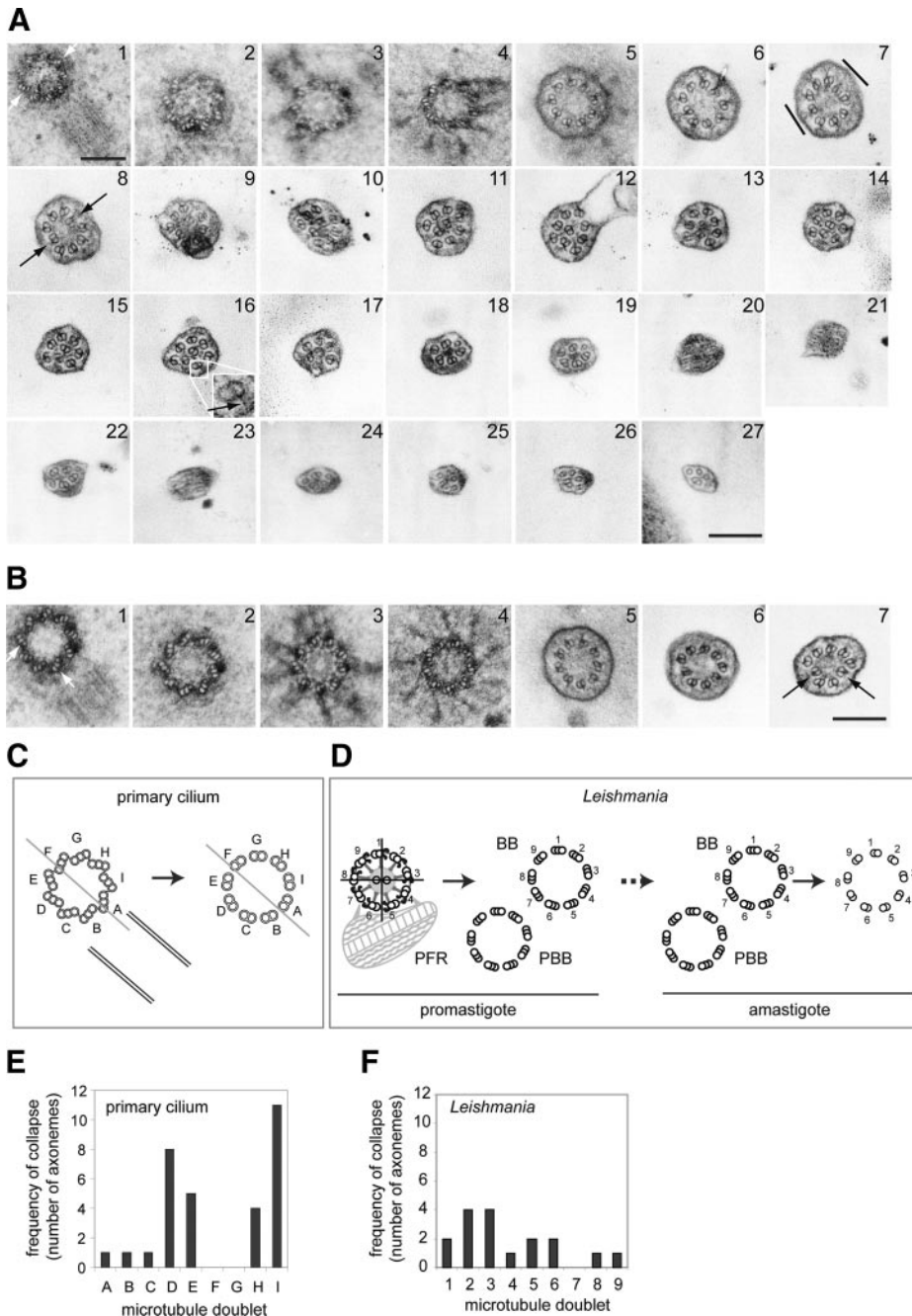


**Figure 2.** Displacement of doublet microtubules in kidney primary cilia and *L. mexicana* flagella. *A, B*) IMCD3 cells were processed for TEM as described previously (22). Numbers indicate adjacent serial sections along the IMCD3 primary cilium. Proximally, the axoneme is 9 + 0 (*A*). Flattening (*A7*, lines) is the first sign of doublet displacement (*A8, B7*; arrows). The doublet-membrane connections remain for much of the cilium length (e.g., *A16*, inset, arrow). *C–F*) Mapping doublet displacement in primary cilia (*C, E*) and *L. mexicana* (*D, F*). *C*) The basal body-procentriole pair with letters (A–I) assigned to each triplet relative to procentriole position; these positions were followed (arrow) through each series. *D*) Absolute doublet and triplet numbering show that the *L. mexicana* promastigote probasal body (PBB) is always adjacent to basal body (BB) triplet 7. These numbers were translated onto the amastigote BB/PBB pair (dashed arrow) and their positions followed as in *C, E, F*). The frequency of doublet displacement observed for each doublet in 18 primary cilium axonemes (*E*; 2 doublets were displaced simultaneously in 14 axonemes) and in 11 amastigote axonemes (*F*; 2 doublets were displaced simultaneously in 6 axonemes). Scale bars = 200 nm.

9). Consequently, the position of the probasal body relative to the basal body was mapped by serial TEM of promastigote flagella. We found that the probasal body is always positioned adjacent to triplet 7 (Fig. 2*D*), an observation that has implications for basal body morphogenesis and inheritance. Assuming an identical positioning of the probasal body in the amastigote, this enabled us to determine which specific doublets were displaced *via* serial section TEM and tomography from the basal body to the flagellum tip in 11 flagella (Fig. 2*D, F* and Supplemental Fig. 1). Displacement was not restricted to a specific doublet; 8 of the 9 doublets were found to be displaced (Fig. 2*F*), suggesting essentially stochastic behavior.

Axoneme collapse occurs early, even during exten-

sion, as evidenced by the structure of a new, still elongating flagellum in a dividing amastigote (Fig. 1*H*). Almost all 9 + 2 cilia and flagella are built and maintained by intraflagellar transport (IFT; ref. 10). In the *L. mexicana* amastigote, we observed IFT-like particles throughout the flagellum (Fig. 1*B*; Supplemental Fig. 1, arrowheads). Although we did not observe IFT particles along the collapsed primary cilium axoneme, we know from studies of ciliary disease that the primary cilium is also built by IFT (1, 10, 11). Thus a collapsed axoneme is no impediment to IFT.

What mechanistic function could the 9v axoneme architecture serve? One has to recognize that a sensory function is a common attribute of flagella and cilia, including many with canonical 9 + 2 axonemes (12,

13). Force generation for flagellar motility requires a high degree of order that imposes constraints on axoneme structure. Sensory cilia need not, however, be thus constrained. There are several examples of sensory cilia that diverge from the 9 + 0 paradigm. Mammalian olfactory cilia have variable 9 + 2, 9 + 3, or 9 + 4 proximal portions and a more distal collapsed 9 + 0 architecture, tapering to a few singlet microtubules at the tip where the olfactory receptors are located (14). The chemosensory neurons of *Caenorhabditis elegans* have 2 types of cilia, amphid channel cilia, which are 9 + 0 with a 9 singlet microtubule extension at the distal end, and amphid wing cilia, which have a fan-shaped morphology rather than a cylindrical arrangement of microtubules (15). The cases we have studied here represent instances of extreme variation from the symmetric 9 + 2/9 + 0 models. In that context why would these extreme cases of symmetry-breaking architecture appear to correlate with a specialization for a sensory role? The best-studied sensory cilium is that of the kidney. Fluid flow through the kidney tubules is proposed to cause bending of the primary cilium, which activates a mechanosensory cation channel (16). Perhaps reorganization from a ring structure could facilitate bending. It may also create a stripped-down axoneme important for optimizing transport of signaling molecules along the microtubules. A lack of radial spokes could grant greater access to microtubules. In addition, possible secretory functions may be facilitated by a loosened connection between microtubules and the ciliary membrane.

This striking observation of conservation of ciliary structure despite the evolutionary distance between *Leishmania* and mammalian cells invites a hypothesis for a function for the *L. mexicana* amastigote flagellum. The amastigote resides inside the parasitophorous vacuole of the macrophage, and the tip of the flagellum is exposed to the vacuole contents. We propose that this might provide a specialized membrane surface where receptor or transport proteins could be located that sense environmental cues and signal or transport molecules across the parasite cell membrane. It is well established that building of the flagellum depends on specific targeting of proteins to the flagellum and IFT-dependent delivery for assembly into the axoneme and associated structures. Cytoplasmic proteins may also be sorted and targeted specifically to the lumen of the flagellum. Moreover it is likely that lipid and protein composition of the flagellar membrane differs from that of the plasma membrane and flagellar pocket, again implying specific sorting mechanisms, which are less well understood. These mechanisms for compartmentalization of proteins to the amastigote flagellum raises the possibility that it could also be used for targeted secretion of vesicles or luminal content into the host cell vacuole, perhaps in response to a signal. A secretory function for cilia has recently been proposed, based on observations of vesicles derived from the flagellum of the green algae *Chlamydomonas* (17). Remarkably, a close examination of amastigote

position inside the vacuole revealed that they were frequently oriented such that the flagellum tip was closely associated with the parasitophorous vacuole membrane (Fig. 3 and Supplemental Movies 3 and 4). We examined 63 individual amastigote flagella in serial sections (in 60 different vacuoles) and found that the tip of 41 of these flagella (65%) was parasitophorous vacuole membrane associated. No other study has looked at the amastigote flagellum tip in relation to parasite attachment. Generally the evidence in the literature addressing the issue of amastigote cell body region of attachment consists of single micrographs showing a range of attachments (see ref. 18). This may indicate variability or may be a reflection of fixation speed. More concerted studies have found that *L. amazonensis* amastigotes were attached to the vacuole membrane by their posterior pole (19). Indeed, the possibility has been rehearsed that MHC class II molecules could be internalized by the parasite *via* its

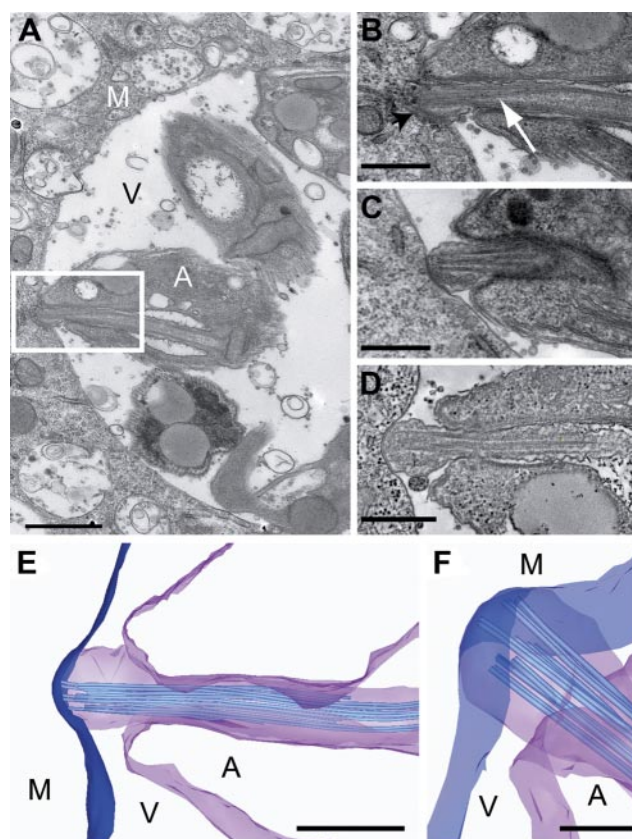


**Figure 3.** The amastigote flagellum is in intimate contact with the parasitophorous vacuole membrane. *A*) Thin section TEM view of *L. mexicana* amastigotes in a J774 macrophage vacuole. *B*) Higher-magnification view of the area delineated by the white box in *A*. Amastigote flagellum tip is closely associated with the vacuole membrane (black arrowhead). White arrow indicates doublet displacement. *C*) Further example of the flagellum-vacuole membrane junction. *D*) Tomographic slice from a reconstructed 3-D volume of an amastigote flagellum in close contact with the vacuole membrane. *E, F*) Tomography model views (23) of the flagellum-vacuole membrane junction. *A*, *L. mexicana* amastigote; *M*, macrophage; *V*, vacuole. Scale bars = 500 nm (*A–E*); 200 nm (*F*).

posterior pole (20), although there is no evidence of such a site being endocytic and much against. The difficulty with all of these studies is the lack of three-dimensional imaging to allow full analysis of the arrangement of the different *Leishmania* species in the parasitophorous vacuole. This will be a major undertaking for the future.

We propose here that receptors on the flagellum tip may bind ligands in the vacuole membrane, triggering signal transduction pathways in the parasite. The structures we observed may even indicate a higher-order organization: perhaps a parasite synapse? Engagement of the flagellum tip with the vacuole membrane could orient the parasite such that signaling and secretion of parasite molecules are precisely targeted to a focal point. In summary, based on structural studies, we propose a hypothesis that the flagellum of the intracellular amastigote parasites is a sensory structure with important and novel functions in maintenance of the host-parasite interaction. This hypothesis is to be tested by molecular and biochemical approaches. **[F]**

We thank Dick McIntosh for comments on the manuscript and David Vaux (University of Oxford, Oxford, UK) for the gift of J774 macrophages. This work was funded by the Wellcome Trust, the Beit Memorial Fellowships for Medical Research, the Jackson Scholarship Fund (Merton College Oxford, to A.E.S.), an EMBO long-term fellowship (to J.L.H.), and the E. P. Abraham Trust. K.G. held a Wellcome Trust Principal Research Fellowship, H.R.D. is a Beit Memorial Fellow, and J.L.H. is a Sir Henry Wellcome Fellow. The Boulder Laboratory for 3D Electron Microscopy of Cells is supported by National Institutes of Health Biotechnology grant RR00592 to A. Hoenger (University of Colorado, Boulder, CO, USA).

## REFERENCES

- Gerdes, J. M., Davis, E. E., and Katsanis, N. (2009) The vertebrate primary cilium in development, homeostasis, and disease. *Cell* **137**, 32–45
- Gull, K. (2009) The parasite point of view: insights and questions on the cell biology of *Trypanosoma* and *Leishmania* parasite-phagocyte interactions. In *Phagocyte-Pathogen Interactions: Macrophages and the Host Response to Infection* (Russell, D. G., and Gordon, S., eds) pp. 453–462, ASM Press, Washington, DC
- Simpson, C. F., Harvey, J. W., and French, T. W. (1982) Ultrastructure of amastigotes of *Leishmania donovani* in the bone marrow of a dog. *Am. J. Vet. Res.* **43**, 1684–1686
- Alexander, J. (1978) Unusual axonemal doublet arrangements in the flagellum of *Leishmania amastigotes*. *Trans. R. Soc. Trop. Med. Hyg.* **72**, 345–347
- Hentzer, B., and Kobayasi, T. (1977) The ultrastructure of *Leishmania tropica* in skin lesions. *Acta Pathol. Microbiol. Scand. B* **85**, 153–160
- Breton-Gorius, J., and Stralin, H. (1967) Formation of rudimentary cilia in primary blood cells of the vitelline sac of rat and chick embryos. *Nouv. Rev. Fr. Hematol.* **7**, 79–94 [in French]
- Allen, R. A. (1965) Isolated cilia in inner retinal neurons and in retinal pigment epithelium. *J. Ultrastruct. Res.* **12**, 730–747
- Dahl, H. A. (1963) Fine structure of cilia in rat cerebral cortex. *Z. Zellforsch. Mikrosk. Anat.* **60**, 369–386
- Gadelha, C., Wickstead, B., McKean, P. G., and Gull, K. (2006) Basal body and flagellum mutants reveal a rotational constraint of the central pair microtubules in the axonemes of trypanosomes. *J. Cell Sci.* **119**, 2405–2413
- Rosenbaum, J. L., and Witman, G. B. (2002) Intraflagellar transport. *Nat. Rev. Mol. Cell. Biol.* **3**, 813–825
- Scholey, J. M., and Anderson, K. V. (2006) Intraflagellar transport and cilium-based signaling. *Cell* **125**, 439–442
- Solter, K. M., and Gibor, A. (1977) Evidence for role of flagella as sensory transducers in mating of *Chlamydomonas reinhardtii*. *Nature* **265**, 444–445
- Shah, A. S., Ben-Shahar, Y., Moninger, T. O., Kline, J. N., and Welsh, M. J. (2009) Motile cilia of human airway epithelia are chemosensory. *Science* **325**, 1131–1134
- Moran, D. T., Rowley, J. C., 3rd, Jafek, B. W., and Lovell, M. A. (1982) The fine structure of the olfactory mucosa in man. *J. Neurocytol.* **11**, 721–746
- Evans, J. E., Snow, J. J., Gunnarson, A. L., Ou, G., Stahlberg, H., McDonald, K. L., and Scholey, J. M. (2006) Functional modulation of IFT kinesins extends the sensory repertoire of ciliated neurons in *Caenorhabditis elegans*. *J. Cell Biol.* **172**, 663–669
- Praetorius, H. A., and Spring, K. R. (2001) Bending the MDCK cell primary cilium increases intracellular calcium. *J. Membr. Biol.* **184**, 71–79
- Baldari, C. T., and Rosenbaum, J. (2010) Intraflagellar transport: it's not just for cilia anymore. *Curr. Opin. Cell Biol.* **22**, 75–80
- Castro, R., Scott, K., Jordan, T., Evans, B., Craig, J., Peters, E. L., and Swier, K. (2006) The ultrastructure of the parasitophorous vacuole formed by *Leishmania major*. *J. Parasitol.* **92**, 1162–1170
- Lang, T., de Chastellier, C., Frehel, C., Hellio, R., Metzereau, P., Leao Sde, S., and Antoine, J. C. (1994) Distribution of MHC class I and of MHC class II molecules in macrophages infected with *Leishmania amazonensis*. *J. Cell Sci.* **107**(Pt. 1), 69–82
- De Souza Leao, S., Lang, T., Prina, E., Hellio, R., and Antoine, J. C. (1995) Intracellular *Leishmania amazonensis* amastigotes internalize and degrade MHC class II molecules of their host cells. *J. Cell Sci.* **108**(Pt. 10), 3219–3231
- Chang, K. P. (1980) Human cutaneous leishmaniasis in a mouse macrophage line: propagation and isolation of intracellular parasites. *Science* **209**, 1240–1242
- Dawe, H. R., Farr, H., Portman, N., Shaw, M. K., and Gull, K. (2005) The Parkin co-regulated gene product, PACRG, is an evolutionarily conserved axonemal protein that functions in outer-doublet microtubule morphogenesis. *J. Cell Sci.* **118**, 5421–5430
- Kremer, J. R., Mastrorade, D. N., and McIntosh, J. R. (1996) Computer visualization of three-dimensional image data using IMOD. *J. Struct. Biol.* **116**, 71–76

Received for publication December 22, 2009.

Accepted for publication March 18, 2010.